

Accepted for publication in ApJ 04/14/2004

**NUMERICAL EXAMINATION OF THE STABILITY OF AN
EXACT TWO-DIMENSIONAL SOLUTION FOR FLUX
PILE-UP MAGNETIC RECONNECTION**

Shigenobu Hirose

*Department of Physics and Astronomy, Johns Hopkins University, Baltimore, MD
21218-2686, USA*

shirose@pha.jhu.edu

Yuri E. Litvinenko

*Institute for the Study of Earth, Oceans, and Space, University of New Hampshire,
Durham, NH 03824-3525, USA*

yuri.litvinenko@unh.edu

Syuniti Tanuma; Kazunari Shibata

Kwasan and Hida Observatories, Kyoto University, Yamashina-ku, Kyoto 607-8471, Japan

tanuma@kwasan.kyoto-u.ac.jp; shibata@kwasan.kyoto-u.ac.jp

Masaaki Takahashi

*Department of Physics and Astronomy, Aichi University of Education, Kariya, Aichi
448-8542, Japan*

takahasi@phyas.aichi-edu.ac.jp

Takayuki Tanigawa

Academia Sinica, Institute of Astronomy and Astrophysics, Taipei 106, Taiwan, R.O.C.

tanigawa@asiaa.sinica.edu.tw

Takahiro Sasaqui

Department of Astronomy, University of Tokyo, Bunkyo-ku, Tokyo 113-0033, Japan

sasaqui@th.nao.ac.jp

Ayato Noro

Department of Physics, Chiba University, Inage-ku, Chiba 263-8522, Japan

`noro@astro.s.chiba-u.ac.jp`

Kazuhiro Uehara

Department of Astronomy, Kyoto University, Sakyo-ku, Kyoto 606-8502, Japan

`uehara@kwasan.kyoto-u.ac.jp`

Kunio Takahashi

Department of Earth Science, Ibaraki University, Mito, Ibaraki 310-8512, Japan

`kutaka@env.sci.ibaraki.ac.jp`

Takashi Taniguchi

Department of Physics, Tokyo University of Science, Shinjuku, Tokyo 162-8601, Japan

`taka0825-0612@mail.goo.ne.jp`

and

Yuliya A. Terekhova

*Institute for the Study of Earth, Oceans, and Space, University of New Hampshire,
Durham, NH 03824-3525, USA*

`yuliya.terekhova@unh.edu`

ABSTRACT

The Kelvin–Helmholtz (KH) and tearing instabilities are likely to be important for the process of fast magnetic reconnection that is believed to explain the observed explosive energy release in solar flares. Theoretical studies of the instabilities, however, typically invoke simplified initial magnetic and velocity fields that are not solutions of the governing magnetohydrodynamic (MHD) equations. In the present study, the stability of a reconnecting current sheet is examined using a class of exact global MHD solutions for steady state incompressible magnetic reconnection, discovered by Craig & Henton. Numerical simulation indicates that

the outflow solutions where the current sheet is formed by strong shearing flows are subject to the KH instability. The inflow solutions where the current sheet is formed by a fast and weakly sheared inflow are shown to be tearing unstable. Although the observed instability of the solutions can be interpreted qualitatively by applying standard linear results for the KH and tearing instabilities, the magnetic field and plasma flow, specified by the Craig–Henton solution, lead to the stabilization of the current sheet in some cases. The sensitivity of the instability growth rate to the global geometry of magnetic reconnection may help in solving the trigger problem in solar flare research.

Subject headings: MHD—plasmas—instabilities—Sun: flares

1. INTRODUCTION

The current consensus is that the explosive release of magnetic energy by virtue of magnetic reconnection in the corona is responsible for the observed solar flares (e.g. Tsuneta 1996; Shibata 1999; Priest & Forbes 2000; Moore et al. 2001). Reconnecting current sheets in the solar corona are believed to form and evolve on the scale of days and weeks, allowing the free magnetic energy in the corona to be accumulated in the sheet. Eventually the sheet is disrupted by an instability, leading to the flare energy release on the scale of minutes and hours.

A well-known difficulty in the flare theory is the so-called trigger problem, which relates to the fact that a relatively slow evolution of the sheet, described by ideal magnetohydrodynamics (MHD), is followed by rapid destabilization when resistive effects in the sheet become important (e.g. Wang & Bhattacharjee 1994; Hirose et al. 2001). The Kelvin–Helmholtz (KH) and tearing instabilities are typically invoked to interpret the transition to the latter stage of the evolution (e.g. Knoll & Chacon 2002; Biskamp 1994, for a review).

Given possible applications to the problem of current sheet evolution and disruption in the solar corona, it is interesting to determine whether the standard results on the KH and tearing instabilities are robust with respect to the influence of the reconnection flow in the sheet and the global geometry of the reconnection solution. This provides the motivation for the present work.

A weakness of most previous analyses of the current sheet instabilities is that they assumed an initial unperturbed state that was not a solution to the resistive steady MHD equations. Previous studies typically assumed a “quasi-equilibrium” one-dimensional tanh-like profile of magnetic field either with zero velocity (Malara et al. 1991, 1992; Dahlburg

et al. 1992) or with a one-dimensional velocity proportional to the magnetic field (Dahlburg & Einaudi 2001). Effects of the plasma flow and the resistive diffusion were not exactly balanced for these initial conditions unless a nonuniform electric resistivity in the sheet was postulated (Schumacher & Seehafer 2000). Left alone, such current sheet would resistively decay. One might also argue that heuristic one-dimensional models for the unperturbed magnetic and velocity field could only describe the immediate vicinity of the current sheet rather than a global MHD solution for magnetic reconnection. We are aware of one work in which the unperturbed state is an exact solution of MHD equations with a uniform and constant electric resistivity: Phan & Sonnerup (1991) investigated linear stability against tearing mode of a one-dimensional current sheet supported by a stagnation-point flow in the plane perpendicular to the magnetic field vector.

In this paper, we use MHD simulations to examine the stability of a reconnecting current sheet described by an exact two-dimensional solution for magnetic reconnection (Craig & Henton 1995). The Craig–Henton solution provides analytical description of flux pile-up magnetic reconnection in incompressible plasma of arbitrary uniform electric resistivity. The resistive diffusion is exactly balanced by a sheared stagnation-point flow, so that steady-state MHD equations are satisfied globally. Notably, we limit consideration to two-dimensional instabilities of the Craig–Henton solution, although previous studies indicated that three-dimensional ideal instabilities of two-dimensional current sheets can grow much faster than any two-dimensional instabilities (e.g. Schumacher & Seehafer 2000; Dahlburg et al. 1992).

Recall that flux pile-up current sheets have been repeatedly studied and generalized not only in two but also in three dimensions (e.g. Craig et al. 1995; Litvinenko & Craig 2000). It is understood that both the Craig–Henton solution and those considered by Sonnerup & Priest (1975) and Phan & Sonnerup (1991) are particular cases of a general family of solutions for flux pile-up merging and reconnection. The analytical nature of the solutions made it possible to demonstrate explicitly many of the characteristics of magnetic reconnection, such as the appearance of small length scales defined by resistivity, magnetic sling shots, and Alfvénic outflows (e.g. Litvinenko & Craig 1999, 2000). It is worth stressing that, although the pile-up reconnection solution is locally equivalent to the Sweet–Parker current sheet as far as reconnection scalings with resistivity are concerned, the two models are not identical globally. The Sweet–Parker model postulates a uniform advection region outside the current sheet, whereas the Craig–Henton solution explicitly describes the magnetic field amplification caused by the non-uniform velocity field outside the sheet.

The paper is organized as follows. In Section 2, we briefly review the steady-state flux pile-up reconnection solutions in two dimensions and identify two types of the solutions depending on the sign of a plasma velocity component at the boundary. In Section 3, we

present the numerical methods for examining the stability of the solutions and describe the numerical results. We compare the results with predictions of the linear theory of the KH and tearing instabilities, discuss the limitations of the local approach and suggest possible solar applications in Section 4. We summarize in Section 5.

2. REVIEW OF THE EXACT FLUX PILE-UP RECONNECTION SOLUTION

We begin by reviewing the Craig–Henton solution that satisfies the steady-state equations of incompressible non-viscous resistive MHD in a planar geometry. Using the Poisson bracket $[\psi, \phi] \equiv \psi_x \phi_y - \psi_y \phi_x$, the non-dimensionalized basic equations can be written as

$$[\nabla^2 \phi, \phi] = [\nabla^2 \psi, \psi], \quad (1)$$

$$E + [\psi, \phi] = \eta \nabla^2 \psi, \quad (2)$$

where ψ and ϕ are, respectively, a flux function for the magnetic field $\mathbf{B} = \nabla \times \psi \hat{\mathbf{z}}$ and a stream function for the velocity field $\mathbf{v} = \nabla \times \phi \hat{\mathbf{z}}$. The problem is specified by two dimensionless parameters E and η . The uniform electric field E , normalized by $v_A B_0$ (in electromagnetic units), characterizes the reconnection rate. The inverse Lundquist number $\eta = \eta_0 / (v_A L)$ is based on a uniform magnetic diffusivity η_0 . Here and in what follows, B_0 , ρ_0 , and L are the reference values of the magnetic field, plasma density, and spatial length scale, $v_A = B_0 / \sqrt{4\pi\rho_0}$ is the reference Alfvén speed.

An exact reconnection solution satisfying the equations above is given by

$$\mathbf{B}(x, y) = (\beta x, -\beta y) + \left(0, -\frac{E}{\eta\mu} \text{daw}(\mu x) \right), \quad (3)$$

$$\mathbf{v}(x, y) = (\alpha x, -\alpha y) + \left(0, -\frac{\beta E}{\alpha \eta\mu} \text{daw}(\mu x) \right), \quad (4)$$

where $\text{daw}(x) \equiv \int_0^x \exp(t^2 - x^2) dt$ is the Dawson function, and the dimensionless parameters α and β define, respectively, the amplitude and the shear of the velocity field (Craig & Henton 1995). These parameters are used to define μ according to

$$\mu^2 = \frac{\beta^2 - \alpha^2}{2\alpha\eta}. \quad (5)$$

Clearly α and β should satisfy $(\beta^2 - \alpha^2)/\alpha > 0$ for the physically interesting case of a localized current sheet, in which case the sheet thickness scales as μ^{-1} .

The distribution of plasma pressure,

$$p(x, y) = p_0 - \frac{1}{2} \left(\alpha^2 (x^2 + y^2) + \left(\frac{E}{\eta\mu} \text{daw}(\mu x) \right)^2 \right) - \beta y \frac{E}{\eta\mu} \text{daw}(\mu x), \quad (6)$$

is derived from the original momentum equation

$$(\mathbf{v} \cdot \nabla) \mathbf{v} = -\nabla^2 \psi \nabla \psi - \nabla p, \quad (7)$$

assuming a constant base pressure p_0 .

Equations (3) and (4) demonstrate that both the magnetic field and the velocity field have a stagnation-flow component proportional to $(x, -y)$, and a shear-flow component proportional to $(0, \text{daw}(\mu x))$. The shear width scales as μ^{-1} .

Assuming that $\beta \geq 0$, the solutions are categorized into two groups according to the flow direction along the x -axis at the external boundary: the outflow solutions with $\alpha > 0$ and $\beta > \alpha$ and the inflow solutions with $\alpha < 0$ and $|\alpha| > \beta$. In the outflow solution the flux pile-up is accomplished mainly by the advection of the x -component of magnetic field by the flow parallel to the y -axis. In the inflow solution $\beta = 0$ corresponds to the anti-parallel merging with stagnation flow (Sonnerup & Priest 1975), and $\beta > 0$ describes the fully two-dimensional solution for flux pile-up reconnection, which is also called “reconnective annihilation” (Priest & Forbes 2000).

Viscous effects, ignored in the solution above and hence throughout this paper, are likely to be important in the region of high shear coinciding with the current sheet. This is potentially more important for the outflow solution that is characterized by a strong velocity shear. The Craig–Henton formalism has been generalized to include viscosity by Fabling & Craig (1996). The latter solution is more complex mathematically. This is why in this paper we concentrate on a simpler non-viscous case in which a simple analytical expression for the initial state is available. Although viscosity effects are neglected without much justification in the outflow case, we wish to stress from the outset that the neglect is justified much better in the inflow case when the flow is only weakly sheared. As we show in Section 4.4, it is the inflow case that is of primary interest to us in the solar flare context. The inflow solution can be tearing unstable, which may explain flare energy release by tearing-induced reconnection.

3. NUMERICAL EXAMINATION OF THE STABILITY OF THE EXACT SOLUTIONS

Typical solutions in the outflow case and the inflow case are shown in Figure 1. As noted in the previous section, a shear of width $2\mu^{-1}$ is present along the y -axis in both the

magnetic and velocity fields. Therefore, we can expect that these solutions can be subject to the KH instability and the tearing instability. We investigated the stability of the solutions using MHD numerical simulations. Specifically we adopted the analytical exact solution as the initial condition, perturbed it slightly, and examined the time development of the system.

3.1. Numerical Method

The basic equations for the numerical simulations are *compressible* resistive MHD equations in the following dimensionless form:

$$\frac{\partial \rho}{\partial t} + \nabla \cdot (\rho \mathbf{v}) = 0, \quad (8)$$

$$\frac{\partial}{\partial t} (\rho \mathbf{v}) + \nabla \cdot \left(\rho \mathbf{v} \mathbf{v} - \mathbf{B} \mathbf{B} + \left(p + \frac{\mathbf{B}^2}{2} \right) \mathbf{I} \right) = 0, \quad (9)$$

$$\frac{\partial \mathbf{B}}{\partial t} + \nabla \times \mathbf{E} = 0, \quad (10)$$

$$\frac{\partial}{\partial t} \left(\frac{1}{2} \rho \mathbf{v}^2 + \frac{p}{\gamma - 1} + \frac{\mathbf{B}^2}{2} \right) + \nabla \cdot \left(\left(\frac{1}{2} \rho \mathbf{v}^2 + \frac{\gamma p}{\gamma - 1} \right) \mathbf{v} + \mathbf{E} \times \mathbf{B} \right) = 0, \quad (11)$$

$$\mathbf{E} = -\mathbf{v} \times \mathbf{B} + \eta \nabla \times \mathbf{B}, \quad (12)$$

where ρ is the plasma density and $\gamma = 5/3$ is the ratio of specific heats. The above equations are normalized in the same way as those in Craig & Henton (1995) and in the previous section, using the reference values of length L , density ρ_0 , and Alfvén speed v_A . The time is normalized with the global Alfvén time $t_A \equiv L/v_A$.

To simulate the Craig–Henton solutions derived for *incompressible* flow, we set the constant base pressure p_0 in equation (6) large enough so that the sound speed is at least ten times greater than both the fluid speed and the Alfvén speed. This ensures that the compressible fluid behaves almost as the incompressible one.

The numerical scheme used in the simulations is based on an upwind scheme with Roe’s numerical fluxes (Powell et al. 1999). Second-order accuracy both in space and time is accomplished by variable extrapolation of Monotone Upstream-centered Schemes for Conservation Laws (MUSCL) and multi-step time integration, guaranteeing Total Variation Diminishing (TVD) with a non-linear limiter function (e.g. Hirsh 1990). Constraint Transport (CT) scheme is combined with the above scheme to develop the magnetic field, ensuring $\nabla \cdot \mathbf{B} = 0$ (Balsara & Spicer 1999).

The simulation box is set to $|x| < 2.5, |y| < 2.5$, and 500×500 constant grids are assigned. This resolution is determined so that at least ten grids are assigned in the current

sheet thickness. The analytical solutions of Craig & Henton (1995) are adopted as the initial conditions for the velocity, magnetic field, and pressure. The initial dimensionless density is set to unity: $\rho(x, y, 0) = 1$. In addition, a small random velocity perturbation (1% of the typical Alfvén velocity v_A) is added in the region of $|x| < 1, |y| < 1$. The inverse Lundquist number is uniform and constant: $\eta(x, y, t) = \eta$. The boundary values are fixed to the initial values for the whole simulation time. The base dimensionless pressure p_0 is fixed at $5 \cdot 10^4$ in all cases. The simulations are performed with the fixed Courant number of 0.8, and the corresponding number of time steps required for a typical run is of order 10^5 .

As far as the accuracy of the numerical method is concerned, we verified that the density fluctuations in the simulation are typically of order 0.01% and never exceed 0.54%. The typical value of $\nabla \cdot \mathbf{v}$, normalized by the ratio of the sound speed and the grid size, is of order 10^{-4} , which is consistent with the magnitude of density fluctuations. Therefore the above value for the base pressure p_0 is indeed large enough to mimic the incompressible behavior. We also confirmed that the compressible code can maintain the unperturbed equilibrium for stable cases. Additionally we performed convergence tests for several cases and confirmed that the stability does not depend on the resolution.

3.2. Overview of the Numerical Results

Parameters of the solutions of which we examined the stability are summarized in Table 1. In Table 1 and hereafter, we adopt the Alfvén time $T_A \equiv L/V_A$ for the normalization of time; T_A is *defined in each case* based on the Alfvén speed V_A at the entrance to the current sheet. This normalization allows us to separate the instability effects under study from amplification of magnetic field carried by the reconnection flow. The relation between T_A and $t_A = L/v_A$ used in the normalization of the basic equations is

$$\frac{T_A}{t_A} = \frac{v_A}{V_A} \approx \frac{\mu\eta}{E}, \quad (13)$$

since v_A is the Alfvén speed at the location where the magnitude of the magnetic field in equation (3) is unity. Here we have defined V_A ignoring a factor ≈ 0.5 , which is the maximum value of the Dawson function, for simplicity.

The growth of the system in each case is summarized in Figure 2. We quantify the perturbation of the velocity distribution in the sheet by plotting the time evolution of

$$I(t') \equiv \log \left(\frac{\iint_{|x| < \mu^{-1}, |y| < 2} |\mathbf{v}(x, y, t') - \mathbf{v}(x, y, 0)| dx dy}{\iint_{|x| < \mu^{-1}, |y| < 2} dx dy} \right), \quad (14)$$

where t' is the time normalized by T_A . The duration of the simulation is $0 < t' < 5$ for the

outflow solutions and $0 < t' < 50$ for the inflow solutions. We stopped the simulations before the evolution of the system could be affected by the fixed boundary conditions.

Figure 2 shows that a choice of parameters leads to instability of both the outflow and the inflow solutions. The nature of the detected instability is, however, entirely different for the two types of solutions. This can be clearly seen in Figure 3, in which the time evolution of some typical *unstable* solutions in both cases is shown. In the outflow solutions (Fig. 3 (a)(b)), the current sheet along the y -axis is warped, and then vortices with magnetic islands are formed, suggesting that the KH instability occurs. On the other hand, in the inflow solutions (Fig. 3 (c)(d)), the time development of the current distribution is symmetric with respect to the y -axis, and long and narrow magnetic islands are formed, which are characteristic features of the tearing instability.

The difference of the unstable behavior comes from the fact that the velocity shear is stronger than the magnetic shear in the outflow solutions, $\beta > \alpha$, and vice versa in the inflow solutions, $\beta < |\alpha|$ (see the terms multiplying the Dawson function in eqs. [3] and [4]). These features can be seen in Figures 4 and 5, which show the distributions of the ratio of the kinetic energy to the magnetic energy. In the outflow (inflow) solutions, the kinetic (magnetic) energy is dominant near the current sheet.

4. INTERPRETATION OF THE NUMERICAL RESULTS

In this section, we discuss the parameter dependencies of the instabilities on the basis of the standard linear theories of the KH instability for the outflow solutions and the tearing instability for the inflow solutions. We also point out that the standard results, derived for uniform initial conditions outside the current sheet, have limited applicability to the pile-up solutions, characterized by strongly nonuniform profiles of the magnetic and velocity fields outside the sheet.

4.1. KH Instability of the Outflow Solution

The standard linear growth rate ω for the KH instability is given by the following expression (Chandrasekhar 1981; Michael 1955):

$$\omega = k \sqrt{\left(\frac{\Delta U}{2}\right)^2 - V_A^2}, \quad (15)$$

where k is the wave number, V_A is the local Alfvén speed, and ΔU is the difference in plasma velocities at the opposite edges of the sheet. Note that Chandrasekhar (1981) discussed in detail the case of a uniform magnetic field whereas Michael (1955) allowed for different magnetic field strengths on the two sides of a discontinuity. The expressions for ω are identical, however, if the magnetic field is symmetrical on either side of the current sheet, which is the case for the Craig–Henton solution.

When applying the formula for the instability growth rate to the Craig–Henton solution, it should be remembered that a continuous velocity profile has the effect of limiting the KH instability to large wave lengths, so that the most unstable mode has k of order the inverse of the sheet thickness l (Chandrasekhar 1981). In this case, since $l = L/\mu$,

$$k_{\max} = \mu/L. \quad (16)$$

Recalling equations (4) and (13), it is straightforward to determine the maximum dimensionless linear growth rate:

$$\omega_{\max} t_A = (k_{\max} L) \sqrt{\left(\frac{\Delta U/2}{v_A}\right)^2 - \left(\frac{V_A}{v_A}\right)^2} = \mu \sqrt{\left(\frac{\beta E}{\alpha \eta \mu}\right)^2 - \left(\frac{E}{\eta \mu}\right)^2} = \frac{E}{\eta} \frac{\sqrt{\beta^2 - \alpha^2}}{\alpha}. \quad (17)$$

The corresponding growth rate normalized with T_A (see eq. [13]) is given by

$$\omega_{\max} T_A = \omega_{\max} t_A \frac{T_A}{t_A} = \frac{\beta^2 - \alpha^2}{\sqrt{2\alpha^3 \eta}}. \quad (18)$$

Linear theory predicts that, in order to overcome the stabilizing effect of the magnetic field, the shear has to be large enough, $\beta > \alpha$, which is the case for the outflow solution.

A major difference between the geometry of the standard KH instability and the outflow Craig–Henton solution is the strongly nonuniform profile of the reconnecting magnetic field and the associated presence of the current sheet at the surface $x = 0$. The stabilization condition, however, should not depend on whether or not the magnetic field is uniform. In fact it is clear on physical grounds that in either case the solution is stable as long as the average Alfvén speed exceeds the fluid velocity difference (e.g. Biskamp 2003). On the other hand, we will see below that the growth rate of unstable solutions can be strongly modified by the global nonuniformity of the field outside the current sheet.

Note that the resistivity in our simulations is small enough for the time scale of the instability $(\omega_{\max})^{-1}$ to be shorter than the diffusion time scale τ_d over the current sheet thickness l . The diffusion time scale is defined as $\tau_d = l^2/\eta_0$ or $\tau_d/T_A = E/(\mu^3 \eta^2)$ in the dimensionless form. The ratio of τ_d/T_A to $(\omega_{\max} T_A)^{-1}$ is typically several tens, and its smallest value is 5.77 in Cases C and D.

The dimensionless wave lengths of the fastest growing modes in the unstable cases can be explained by the linear theory, but the growth rates are smaller by an order of magnitude, compared with the predicted values in Table 1. For example, in Case B, the fastest growing mode has the wave length of ≈ 0.5 (see Fig. 3(a): $t' = 3.0$), which agrees with the value predicted by the linear theory ($= 0.51$), while the growth rate (≈ 2.7) is much smaller than the predicted value ($= 21.21$). One factor that may be responsible for this significant reduction in the growth rate is the magnetic field gradient outside the sheet, which is associated with the reverse electric current in the Craig–Henton solution. The magnetic field pile-up on either side of the current sheet corresponds to the field variation of order $\sim E/(\eta\mu)$ over the length scale $\sim \mu^{-1}$ (eq. [6]). Since the corresponding energy density $\sim (E/(\eta\mu))^2$ is comparable to the kinetic energy of the shearing motion (eq. [4]), the KH instability may be suppressed by the nonuniform magnetic field outside the sheet.

4.2. Tearing Instability of the Inflow Solution

The maximum growth rate of the tearing instability and the corresponding wave number are given by the following formulas, ignoring factors of order unity (Furth, Killeen, & Rosenbluth 1963):

$$\omega_{\max} = \frac{1}{\sqrt{\tau_d \tau_A}}, \quad (19)$$

$$k_{\max} = \left(\frac{\tau_A}{\tau_d} \right)^{\frac{1}{4}} \frac{1}{l}, \quad (20)$$

where $\tau_d = l^2/\eta_0$ and $\tau_A = l/V_A$ are the diffusion and Alfvén time scales in the current sheet of thickness l . Using equations $\eta = \eta_0/(v_A L)$, $l/L = 1/\mu$, and (13), we have the following expressions for the dimensionless linear growth rate and wave number for the tearing instability:

$$\omega_{\max} t_A = \sqrt{\frac{V_A}{v_A} \frac{\eta_0}{v_A L} \left(\frac{L}{l} \right)^3} = \sqrt{\frac{E}{\eta\mu} \eta\mu^3} = \sqrt{\frac{(\beta^2 - \alpha^2) E}{2\alpha\eta}}, \quad (21)$$

$$k_{\max} L = \left(\frac{\eta_0}{L v_A} \frac{L}{l} \frac{v_A}{V_A} \right)^{\frac{1}{4}} \frac{L}{l} = \left(\eta\mu \frac{\mu\eta}{E} \right)^{\frac{1}{4}} \mu = \left(\frac{(\beta^2 - \alpha^2)^3}{8\alpha^3 \eta E} \right)^{\frac{1}{4}}, \quad (22)$$

where it should be remembered that $\alpha < 0$ and $\beta < |\alpha|$. The corresponding growth rate normalized with T_A is

$$\omega_{\max} T_A = \omega_{\max} t_A \frac{T_A}{t_A} = \frac{\alpha^2 - \beta^2}{2|\alpha|\sqrt{E}}. \quad (23)$$

Thus stronger inflows (large α) and weaker two-dimensionality (small β) are the factors that make the current sheet more unstable with respect to tearing. Theory demands that λ_{\max}/l be greater than 2π for the instability, which is the case for the inflow solutions (see Table 1).

The analytical estimate for $\omega_{\max}t_A$ ignores the effect of the reconnection flow on the instability. It is easy to see on physical grounds that a strong flow would carry the growing modes out of the reconnection region, thus suppressing the instability (see Biskamp 1994, and references therein). A rough condition for such stabilization is simply $|\alpha| > \omega_{\max}t_A$, which becomes

$$\frac{|\alpha|}{1 - \beta^2/\alpha^2} > \frac{E}{\eta} \quad (24)$$

for the flux pile-up reconnection solution under consideration. For typical simulation parameters, however, this condition is difficult to achieve unless $\beta \rightarrow |\alpha|$, indicating a broad current sheet extending to the external boundaries.

Chen & Morrison (1990) and Ofman et al. (1991) studied the influence of the velocity shear on the tearing instability and found that the instability is suppressed when the flow shear is larger than the magnetic field shear at the neutral plane. It is worth remarking that the flow geometry assumed in our study is different. Recall that the inflow Craig–Henton solution is defined by a weak shear, specifically $\beta < |\alpha|$. This condition is required in order to have a localized current sheet (see Section 2). Another difference with the problem investigated by Chen & Morrison (1990) is that the Craig–Henton solution possesses the reconnection outflow that also have a stabilizing effect. There is a formal similarity between stabilization by the velocity shear and the reconnection outflow, although the flow geometry is different. One also should remember that when the flow shear is large, the behavior of the reconnecting current sheet is more complex because it is no longer easy to distinguish the effects of the tearing and KH instabilities, and both effects are generally present (Ofman et al. 1991).

Both the wave lengths and the growth rates in the unstable cases can be basically explained by the linear theory. For example, in Case K, the fastest growing mode has the wave length of ≈ 2.5 (see Fig. 3(c): $t' = 25.0$) and the growth rate of ≈ 0.3 , which agree fairly well with the values predicted by the linear theory ($\lambda_{\max}/L = 3.51$ and $\omega_{\max}T_A = 0.33$). Furthermore, comparing (c) and (d) in Figure 3, the fastest growing mode in Case N has a shorter wave length and a larger growth rate than that in Case K, which is also consistent with the linear theory (see Table 1).

4.3. Effects of Nonuniform Initial Conditions

Equations (18) and (23) predict that the KH instability occurs in the outflow solutions ($\beta > \alpha$) and the tearing instability occurs the inflow solutions ($\beta < |\alpha|$) for any values of the parameters, α , β , E , and η . The instabilities in our simulations can be interpreted using the standard linear theories. We found, however, that the Craig–Henton solution is stable for some values of the parameters. This indicates that the standard linear results, based on uniform initial conditions, are of limited use when analyzing the stability of global nonuniform MHD solutions.

In the application of linear theories to the solutions discussed above, we used the values of the velocity and magnetic field at the entrance to the current sheet. The solutions at hand, however, are neither one-dimensional nor uniform. We expect that, if the length scale of one-dimensionality is not large enough compared with the wave length for the most unstable mode, the instabilities will be modified owing to the resulting interaction with the external fields. In Figure 4 (Figure 5), the dark (light) color region outside the current sheet is the region where the KH (tearing) instability will be influenced by the external fields, since the magnetic (kinetic) energy is dominant there. For example, in Case F, the kinetic-energy dominant region (light color region) is smaller than that in Case B, and thus the KH instability occurs in a smaller region compared with Case B (see Fig. 3 (a)(b)).

It may be argued, therefore, that the instabilities can be suppressed when the effects of two-dimensionality and nonuniformity, ignored in the standard treatment, become important in the initial configuration. Equations (3) and (4), describing the structure of the Craig–Henton solution, can be used to quantify the expected effect. The two-dimensional magnetic field in the outflow solution, for example, should start influencing the shearing velocity profile when the first term of equation (3) becomes large compared with the second term of equation (4), that is when α increases (Case H), E decreases (Case C), or η increases (Case D). This may explain why cases C (small E) and D (large η) in the outflow solution appear to be stable. A similar argument can be given for the inflow solution by comparing the first term of equation (4) and the second term of equation (3). The two-dimensionality should come into play when α increases (Case Q), η increases (Case M), or E decreases (Case L). Perhaps this is why we did not detect instability in cases L (small E), M (large η), and Q (large α) in the inflow solution.

The lack of instability in cases L, M, and Q is also consistent with the qualitative equation (24). Interestingly, it appears that this order-of-magnitude stability condition can be made quantitative if its left-hand side is multiplied by a factor of order 10^2 . Recall that a similarly large factor for the aspect ratio of a dynamic Sweet–Parker current sheet, stable with respect to tearing, was suggested by Biskamp (1994).

4.4. Tearing in the Solar Corona

This work is partly motivated by the idea that tearing of a large-scale current sheet in the solar corona can lead to impulsive energy release in solar flares (e.g. Sturrock 1994). The flux pile-up solution investigated in this paper is a member of the only exact analytical MHD family of solutions for magnetic reconnection that we are aware of, and analytical scalings based on these solutions may be of general interest. One important question is whether the growth rate of the tearing mode is sufficiently rapid if the realistic electric resistivity in the solar corona is assumed. Our numerical results are in quantitative agreement with the linear theory of tearing instability as long as the stabilizing effects of two-dimensional geometry are small enough. We now proceed to show that the instability scalings do imply the possibility of rapid conversion of magnetic energy in a large-scale current sheet in the corona.

The time-scale of destabilization, caused by tearing of a current sheet, is conveniently defined as $\tau = \omega_{\max}^{-1}$. As discussed above, our simulations confirm that the growth rate for the flux pile-up solution ω_{\max} can be estimated using equation (21). While solar observations put some constraints on the dimensions of reconnection regions, reconnection rates, and the electric resistivity, the observations are not detailed enough to specify the geometry of reconnective flows, given by the parameters α and β . This is why, in order to apply the formula for ω_{\max} to unstable current sheets in solar active regions, we rewrite equation (21) as follows:

$$\frac{\tau}{t_A} = \frac{S^{1/2}}{\tilde{B}_s^{1/2}} \left(\frac{l}{L} \right)^{3/2}, \quad (25)$$

where $S = \eta^{-1}$ is the Lundquist number, and the dimensionless pile-up factor $\tilde{B}_s = V_A/v_A$ is simply the magnetic field at the entrance to the sheet relative to the reference value B_0 . This equation for τ reduces to the standard result for tearing in the Sweet–Parker current sheet, provided the pile-up is absent, in which case $\tilde{B}_s = 1$ and $l/L = S^{-1/2}$.

Adopting $L = 10^{9.5}$ cm, $B_0 = 10^2$ G, and $v_A = 10^9$ cm s⁻¹ as the reference values in a solar active region, we can estimate $S \approx 10^{14}$ based on the classical value of electric resistivity. Models for the structure of flaring current sheets suggest that their thickness is unlikely to exceed $l \approx 10^5$ cm (e.g. LaRosa 1992; Litvinenko & Craig 2000), which leads to $l/L \approx 10^{-4.5}$. Coronal magnetic fields are unlikely to exceed 10^3 G, hence we should assume a modest pile-up factor $\tilde{B}_s \approx 10$. These numerical values result in the instability time-scale of order the Alfvén time $t_A \approx 10^{0.5}$ s. Although nonlinear effects eventually come into play, this estimate for τ confirms that pile-up current sheets can be unstable to tearing and can be destroyed quite rapidly in the corona. This conclusion should remain qualitatively valid if current-driven instabilities give rise to plasma turbulence and enhanced electric resistivity in the sheet. Although the sheet should thicken up due to increased resistivity, this effect

will be partly balanced by the corresponding decrease in the effective Lundquist number.

A relevant question at this point is whether flux pile-up reconnection solutions adopted for our simulations are possible in the solar corona at all. It might be argued that, since the Craig–Henton solution is unstable for a wide range of parameters, it is not realized on the Sun. We wish to stress, however, that the simulations also identified a parameter regime in which the Craig–Henton solution is stable. In particular the stability with respect to tearing in cases L, M, and Q is consistent with the qualitative stabilization condition given by equation (24). The stability appears to be intimately related to the two-dimensionality of the solution. Equation (24) indicates that instability is easier to achieve when $\beta \rightarrow 0$, which corresponds to one-dimensional merging of magnetic fields. The shear parameter β would be difficult to determine observationally. As in our estimate for τ , however, we can eliminate β in equation (24) by specifying the current sheet thickness l . In order to give an illustrative example, we assume $\alpha \approx 1$ and $l \approx 10^6$ cm. Then the stabilization condition can be written as $E < (l/L)^2 \approx 10^{-7}$, which corresponds to $E < 10^{-4}$ V cm $^{-1}$ in dimensional units. We suggest that stable two-dimensional solutions can describe relatively thick (large l), slowly reconnecting (small E), stable current sheets in the solar corona.

Finally, based on this sensitivity of our numerical results to the global geometry of magnetic reconnection, it would be tempting to suggest that changes in the geometry of the solution may be responsible for rapid changes in the rate of magnetic energy release by magnetic reconnection and thus may trigger solar flares. One caveat is that we only performed a parametric study of stability of the steady flux pile-up solutions. A rigorous approach to the trigger problem would require the solution of a much more complicated task: we would have to track the dynamical evolution of a current sheet with time-dependent parameters that reflect, for example, a slow change in boundary conditions at the photosphere due to the emergence of magnetic flux and photospheric flows.

5. DISCUSSION

Exact MHD solutions are now available, which describe genuine flux pile-up magnetic reconnection, as opposed to simple one-dimensional merging (Craig et al. 1995). Since these analytical solutions explicitly demonstrate many of the properties of fast reconnection, their analysis can be a powerful tool in the reconnection theory (e.g. Litvinenko & Craig 2000; Heerikhuisen, Litvinenko, & Craig 2002). Furthermore, the solutions are known quantitatively to describe the results of numerical simulations performed using a time-dependent code (Heerikhuisen, Craig, & Watson 2000).

We have examined in this paper the stability of an exact two-dimensional solution for flux pile-up reconnection in incompressible resistive plasma (Craig & Henton 1995). We used numerical simulations to show that the solutions of the outflow type can be Kelvin–Helmholtz (KH) unstable and the solutions of the inflow type can be tearing unstable. Notably, we used the steady Craig–Henton solution as an initial condition, thus allowing enough time for the instability to develop. Our approach should be contrasted with that of a time-dependent simulation (Heerikhuisen, Craig, & Watson 2000) in which a localized current sheet was present for a finite (perhaps insufficient) time in a doubly periodic geometry. Although the latter simulation provided some evidence that the sheet could break up into magnetic islands, it was not clear whether the tearing instability was responsible for the phenomenon.

In the outflow solutions, where a current sheet is formed by strong shearing flows, the KH instability was observed to develop. The numerical results can be qualitatively explained by the standard linear theory of the KH instability (eq. [18]). The absolute values of the growth rates, however, are smaller than those predicted. This may be due to the strongly nonuniform profile of the magnetic field at the entrance to the current sheet. The inflow solutions are characterized by a fast, weakly sheared inflow that leads to a strong magnetic field pile-up and the formation of a localized current sheet. These are the conditions under which the tearing instability is likely to develop. The computed growth rates can be explained fairly well by the standard linear theory of the tearing instability (eq. [23]). The instability, however, is suppressed when the effects of two-dimensionality are large enough to modify the evolution of the flux pile-up current sheets.

Thus the numerical results often can be interpreted by applying standard results for the KH and tearing instabilities to the particular geometries of magnetic field and plasma flow, specified by the Craig–Henton solution. These instabilities cause turbulent and non-steady evolution of the current sheet, which is favorable for fast magnetic reconnection (e.g. Shibata & Tajima 2001; Tajima & Shibata 1997) or particle acceleration (e.g. Litvinenko 2003; Aschwanden 2002). In some cases, however, the global nature of the solution leads to the suppression of the instabilities. Of particular interest is the dependence of the growth rate and the most unstable wave length on the parameters of the reconnection solution: reconnection rate E , resistivity η , reconnection flow amplitude α and shear β . Finally, we note that the sensitivity of the results to the nonuniform profiles of the magnetic and velocity fields in the reconnection region, as well as the effects of two-dimensionality of the solution, may be responsible for rapid changes in the rate of magnetic energy release by magnetic reconnection, which in turn may help in solving the trigger problem in solar flare research.

Numerical computations were carried out on VPP5000 at the Astronomical Data Analysis Center of the National Astronomical Observatory, Japan (project ID: yst15a and hst21a),

which is an inter-university research institute of astronomy operated by Ministry of Education, Science, Culture, and Sports, and on VPP5000 at the Super Computer Center, Nagoya University, by the joint research program of the Solar-Terrestrial Environment Laboratory, Nagoya University. This study was initiated as a part of the ACT-JST summer school for numerical simulation in Astrophysics and Space Plasma. One of the authors (Y.E.L.) acknowledges fruitful discussions with I. J. D. Craig and the support by NSF grants ATM-0136718 and IP-9910067 and NASA grant NAG5-10852.

REFERENCES

- Aschwanden, M. 2002, *Space Sci. Rev.*, 101, 1
- Balsara, D. S., & Spicer, D. S. 1999, *J. Comp. Phys.*, 149, 270
- Biskamp, D. 1994, *Phys. Rep.*, 237, 179
- Biskamp D. 2003, *Magnetohydrodynamic Turbulence* (Cambridge: Cambridge University Press)
- Chandrasekhar, S. 1981, *Hydrodynamic and Hydromagnetic Stability* (New York: Dover)
- Chen, X. L., & Morrison, P. J. 1990, *Phys. Fluids B*, 2, 495
- Craig, I. J. D., & Henton, S. M. 1995, *ApJ*, 450, 280
- Craig, I. J. D., Fabling, R. B., Henton, S. M., & Rickard, G. J. 1995, *ApJ*, 455, L197
- Dahlburg, R. B., Antiochos, S. K., & Zang, T. A. 1992, *Phys. Fluids B*, 4, 3902
- Dahlburg, R. B., & Einaudi, G. 2001, *Phys. Plasmas*, 8, 2700
- Fabling, R. B., & Craig, I. J. D. 1996, *Phys. Plasmas*, 3, 2243
- Furth, H. P., Killeen, J., & Rosenbluth, M. N. 1963, *Phys. Fluids*, 6, 459
- Heerikhuisen, J., Litvinenko, Y. E., & Craig, I. J. D. 2002, *ApJ*, 566, 512
- Heerikhuisen, J., Craig, I. J. D., & Watson, P. G. 2000, *Geophys. Astrophys. Fluid Dynamics*, 93, 115
- Hirose, S., Uchida, Y., Uemura, S., Yamaguchi, T., & Cable, S. B. 2001, *ApJ*, 551, 586

- Hirsh, C., 1990, Numerical Computation of Internal and External Flows (Vol. 2) (Chichester: John Wiley & Sons)
- Knoll, D. A., & Chacon, L. 2002, Phys. Rev. Lett., 88, 215003
- LaRosa, T. N. 1992, ApJ, 396, 289
- Litvinenko, Y. E. 2003, Sol. Phys., 212, 379
- Litvinenko, Y. E., & Craig, I. J. D. 1999, Solar Phys., 189, 315
- Litvinenko, Y. E., & Craig, I. J. D. 2000, ApJ, 544, 1101
- Malara, F., Veltri, P., & Carbone, V. 1991, Phys. Fluids B, 3, 1801
- Malara, F., Veltri, P., & Carbone, V. 1992, Phys. Fluids B, 4, 3070
- Michael, D. H. 1955, Proc. Camb. Phil. Soc., 51, 528
- Moore, R. L., Sterling, A. C., Hudson, H. S., & Lemen, J. R. 2001, ApJ, 552, 833
- Ofman, L., Chen, X. L., Morrison, P. J., & Steinolfson, R. S. 1991, Phys. Fluids B, 3, 1364
- Phan, T. D., & Sonnerup, B. U. Ö. 1991, J. Plasma Phys., 44, 525
- Powell, K. G., Roe, P. L., Linde, T. J., Gombosi, T. I., & De Zeeuw, D. L. 1999, J. Comp. Phys., 154, 284
- Priest, E. R., & Forbes, T. G. 2000, Magnetic Reconnection: MHD Theory and Applications (Cambridge: Cambridge University Press)
- Schumacher, J., & Seehafer, N. 2000, Phys. Rev. E, 61, 2695
- Shibata, K. 1999, Astrophys. Space Sci., 264, 129
- Shibata, K., & Tajima, T. 2001, Earth, Planets, and Space, 33, 473
- Sonnerup, B. U. Ö., & Priest, E. R. 1975, J. Plasma Phys., 14, 283
- Sturrock, P. A. 1994, Plasma Physics: An Introduction to the Theory of Astrophysical, Geophysical, and Laboratory Plasmas (Cambridge: Cambridge University Press)
- Tajima, T., & Shibata, K. 1997, Plasma Astrophysics (Reading: Addison-Wesley)
- Tsuneta, S. 1996, ApJ, 456, 840

Wang, X., & Bhattacharjee, A. 1994, ApJ, 420, 415

Table 1. Parameters of the solutions the stability of which is examined. Cases A to I are outflow solutions ($\alpha > 0$), and Cases J to R are inflow solutions ($\alpha < 0$). The solutions are characterized by the dimensionless electric field E , reconnection flow amplitude α and shear β , and electric resistivity η . L is the global length scale, $l = L/\mu$ is the current sheet thickness, T_A is the Alfvén time based on L and the magnetic field at the entrance to the sheet.

Case		E	α	β	η	μ	$\omega_{\text{num}}T_A^{\text{a}}$	$\omega_{\text{max}}T_A^{\text{b}}$	$\lambda_{\text{max}}/L^{\text{b}}$	$\lambda_{\text{max}}/l^{\text{b}}$
A		0.50	1.0	2.0	0.010	12.25	1.2	21.21	0.51	6.3
B	(large E)	2.00	1.0	2.0	0.010	12.25	2.3	21.21	0.51	6.3
C	(small E)	0.05	1.0	2.0	0.010	12.25	—	21.21	0.51	6.3
D	(large η)	0.50	1.0	2.0	0.100	3.87	—	6.71	1.62	6.3
E	(small η)	0.50	1.0	2.0	0.003	22.36	1.6	38.73	0.28	6.3
F	(large β)	0.50	1.0	3.0	0.010	20.00	1.2	56.57	0.31	6.3
G	(small β)	0.50	1.0	1.5	0.010	7.91	0.7	8.84	0.79	6.3
H	(large α)	0.50	1.3	2.0	0.010	9.42	0.7	11.02	0.67	6.3
I	(small α)	0.50	0.5	2.0	0.010	19.36	2.6	75.00	0.32	6.3
J		1.0	-1.0	0.25	0.005	9.68	0.32	0.47	2.95	28.6
K	(large E)	2.0	-1.0	0.25	0.005	9.68	0.28	0.33	3.51	34.0
L	(small E)	0.2	-1.0	0.25	0.005	9.68	—	1.05	1.97	19.1
M	(large η)	1.0	-1.0	0.25	0.100	2.17	—	0.47	6.24	13.5
N	(small η)	1.0	-1.0	0.25	0.001	21.65	0.32	0.47	1.97	42.7
O	(large β)	1.0	-1.0	0.80	0.005	6.00	0.11	0.18	6.05	36.3
P	(small β)	1.0	-1.0	0.05	0.005	10.00	0.24	0.50	2.82	28.1
Q	(large α)	1.0	-5.0	0.25	0.005	22.33	—	2.49	0.84	18.8
R	(small α)	1.0	-0.4	0.25	0.005	4.94	0.10	0.12	8.10	40.0

^aThe instability growth rates ω_{num} are roughly computed using Fig. 2.

^bIn the outflow case, the predicted growth rate ω_{max} and the wave length for the most unstable mode λ_{max} are those for the KH instability (eqs. [18] and [16]), while in the inflow case, those for the tearing instability (eqs. [23] and [22]).

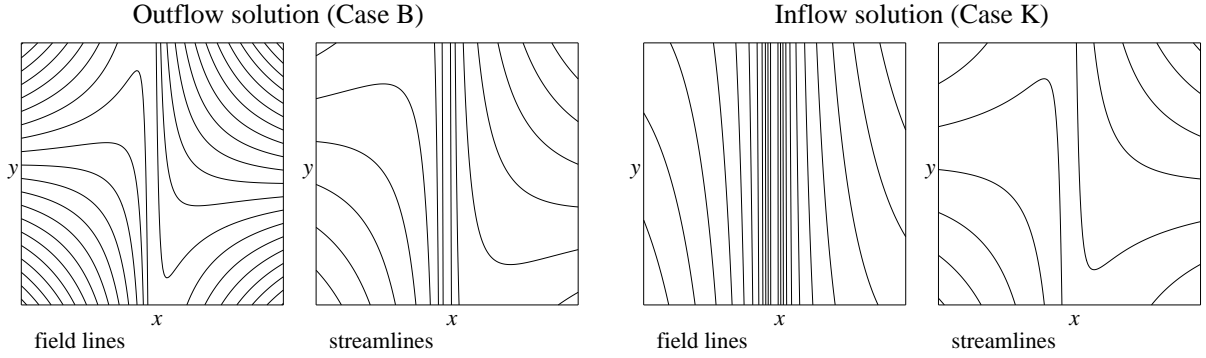


Fig. 1.— Field lines and streamlines of the outflow solution (Case B) and the inflow solution (Case K). The displayed area is $|x| < 2$, $|y| < 2$ (the origin is at the center). The densities of field lines and streamlines correspond to $|\mathbf{B}|$ and $|\mathbf{v}|$, respectively. Parameters of each case are shown in Table 1.

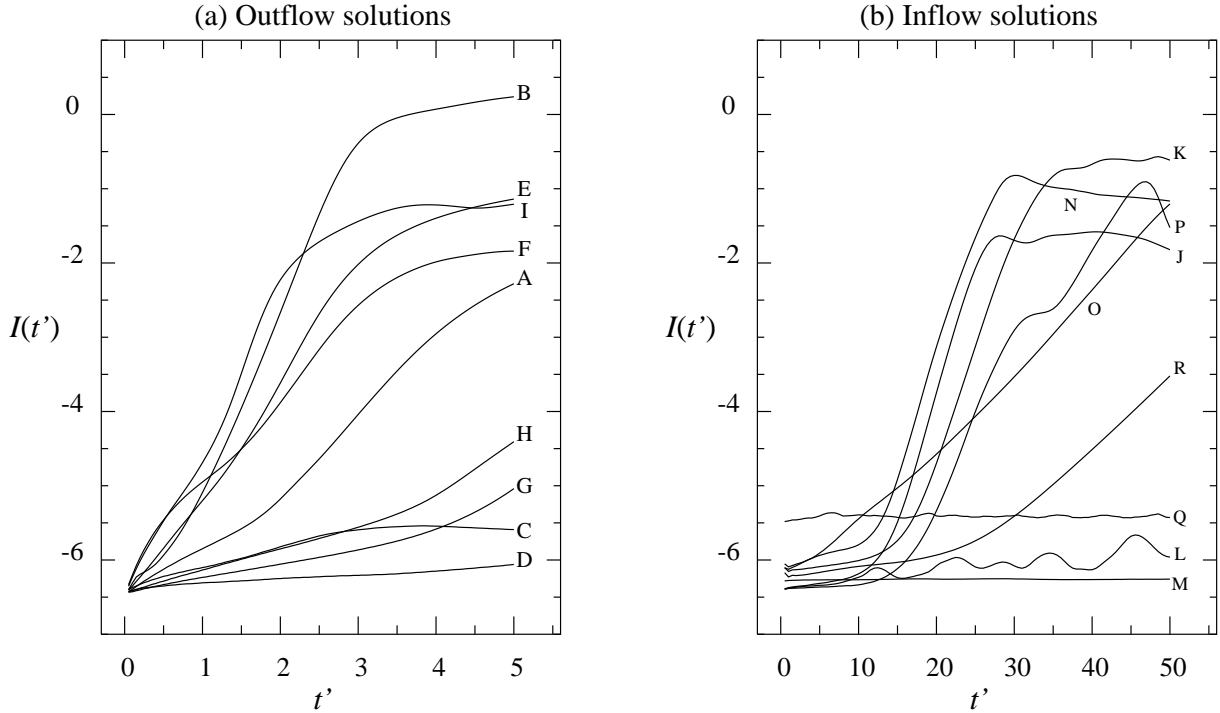


Fig. 2.— The instability growth as measured by $I(t')$ (defined in eq. [14]) in outflow solutions (Case A to I) and inflow solutions (Case J to R). Note that t' is the time normalized with $T_A = L/V_A$.

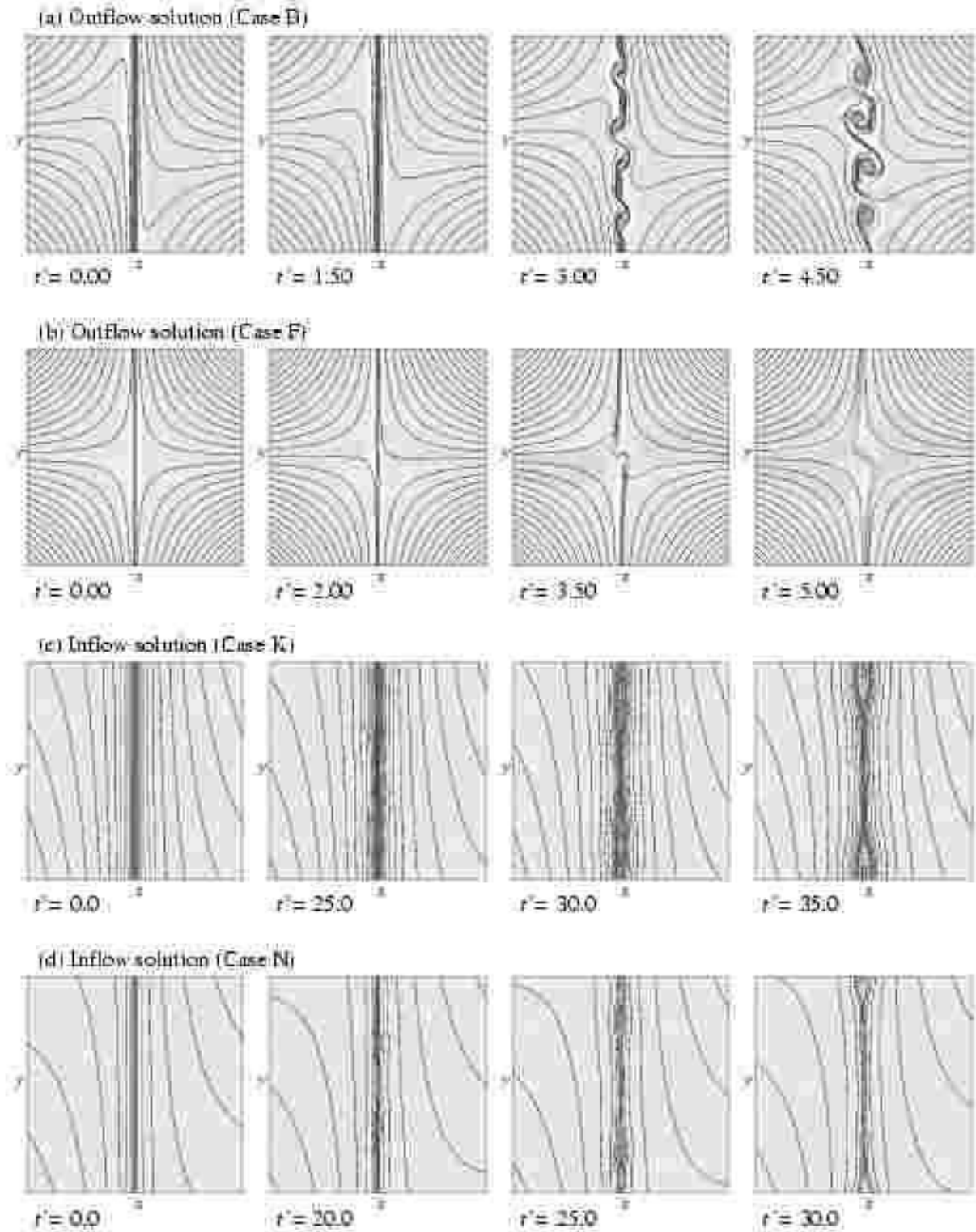


Fig. 3.— Typical time developments of the instabilities for outflow solutions (Cases B and F) and inflow solutions (Cases K and N). Solid lines represent the magnetic field lines. Gray scale represents the z -component of the current density; darker gray corresponds to a larger current density. The displayed area is $|x| < 2, |y| < 2$ (the origin is at the center).

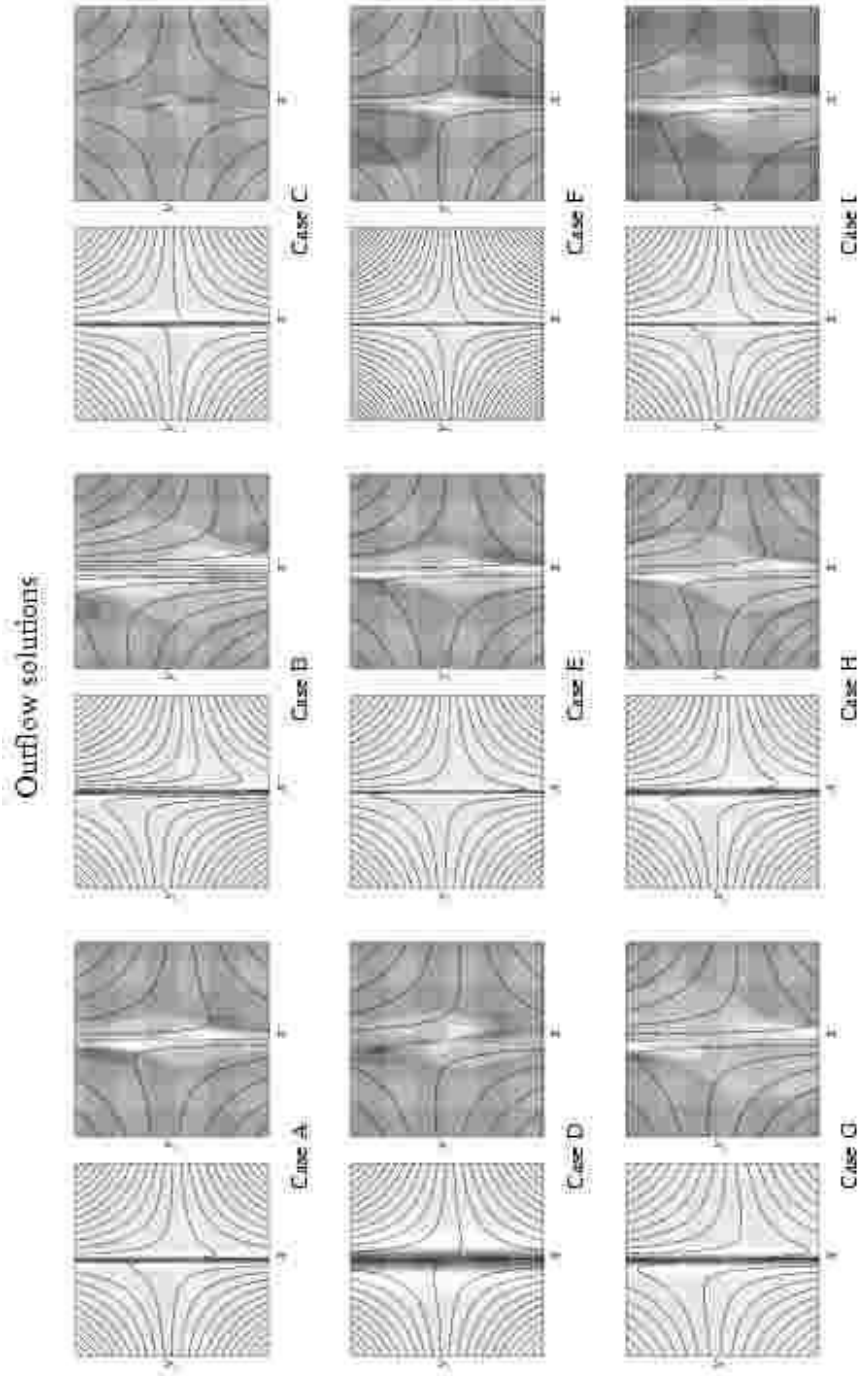


Fig. 4.— Structure of the outflow solutions (Cases A to I). In each case, the left figure shows the distribution of the current density (gray scale) and field lines (solid lines), while the right figure shows the streamlines (solid lines) and $\log_{10}(E_K/E_M)$ (gray scale), where E_K is the kinetic energy and E_M is the magnetic energy. The gray scale in the right figure has six steps, ~ -2 (lightest), $-2 \sim -1$, $-1 \sim 0$, $0 \sim 1$, $1 \sim 2$, $2 \sim$ (darkest). The displayed area is $|x| < 2, |y| < 2$ (the origin is at the center).

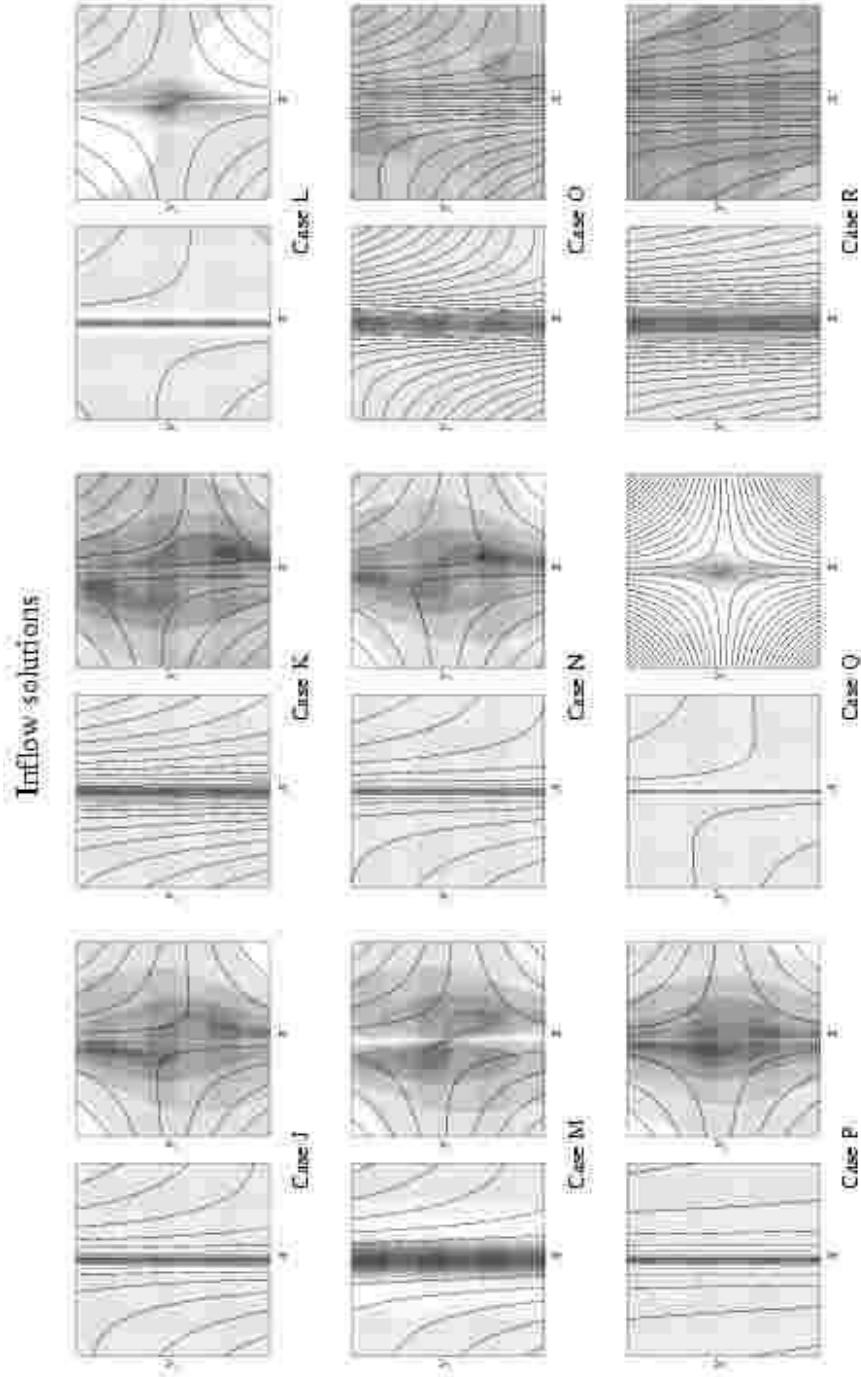


Fig. 5.— Structure of the inflow solutions (Cases J to R). See the caption of Figure 4.